The Specific Work of Flow as a Criterion for Orientation in Polymer Crystallization

Oleksandr O. Mykhaylyk,*,† Pierre Chambon,† Richard S. Graham,‡,§ J. Patrick A. Fairclough,† Peter D. Olmsted,‡ and Anthony J. Ryan†

Department of Chemistry, University of Sheffield, Brookhill, Sheffield S3 7HF, UK; School of Physics & Astronomy, University of Leeds, Leeds LS2 9JT, UK; and School of Mathematical Sciences, University of Nottingham, Nottingham NG7 2RD, UK

Received November 23, 2007
Revised Manuscript Received February 7, 2008

Polyolefins comprise the most widely used class of synthetic polymers, and their conversion into products generally involves shaping a liquid (using a die or a mold) and then stabilizing that shape by crystallization. In the semicrystalline solid state the degree of crystallinity and crystal orientation determines the physical properties and is strongly dependent on processing conditions.[1] The morphology spans a structural hierarchy from molecular (<nm) to just visible (<mm) length scales that is technologically very important and scientifically rather challenging. Flow introduces a profound change from isotropic spherulites to highly oriented "shish kebabs" with a corresponding large increase in stiffness and strength.[2] All industrial polymers have a distribution of molecular species, in terms of both their total length and degree of branching, and the flow-induced morphological transition is particularly sensitive to those chains with the longest relaxation times. The earliest polyolefins had broad molecular weight distributions and long-chain branching, which led to attractive properties.[3] Modern catalyst technology allows control over both stereochemistry and chain topology,[4−7] and to fully take advantage of this, a better understanding of the link between molecules, flow, and properties is needed.[8]

Flow-induced superstructures comprising threadlike cores (shish) decorated by lamellar crystals (kebabs) were first observed in crystals grown from solution.[9,10] Similar oriented structures were soon observed in bulk polymer,[11] but the mechanism of their formation is still unresolved. Flow is responsible for both the orientation of polymer chains, (at shear rates $\dot{\gamma} > 1/\tau_d$, where τ_d is the reptation time) and the stretching of polymer chains (at higher shear rates $\dot{\gamma} > 1/\tau_R > 1/\tau_d$, where τ_R is the longest Rouse time in the melt).[12] While the first condition could be necessary for the formation of an oriented structure,[13,14] the second condition ensures strong stretching of molecules into a conformation ideal for crystallization. This, then, suggests that there is a minimum shear rate $\dot{\gamma}_{min} \sim 1/\tau_R$, below which the orientated nuclei cannot be obtained, and therefore, an oriented structure (shish kebab) is unlikely to be formed in a crystallizing polymer. This trend was noted by van Meerveld and co-workers in an exhaustive literature review.[15] However, this hypothesis is difficult to quantitatively verify on polydisperse materials[13,14] due to their typically broad distribution of relaxation times; the ideal experimental system is thus bidisperse with well-separated time scales.[12] A number of experimental methods can be used for studying crystallzation in shear flow. At one extreme, an extruder[16,17] reproduces industrial processing conditions with a wide distribution of shear rates (from parabolic to pluglike[18]) in a pressure-driven slot flow, and at the other extreme the cone and plate geometry has a uniform shear rate.[19] In the extruder most measurements are averaged across complex flow in the slot, whereas in a cone and plate rheometer a single shear rate is studied. An intermediate situation is the plate−plate geometry, in which the shear rate increases linearly with radius (Figure 1a); thus, one can produce a radial map of properties as a function of shear rate by studying the sample after suitable flow conditions. This "combinatorial" technique can thus be used to measure the critical flow conditions responsible for orienting crystallizing polymers in a single experiment.

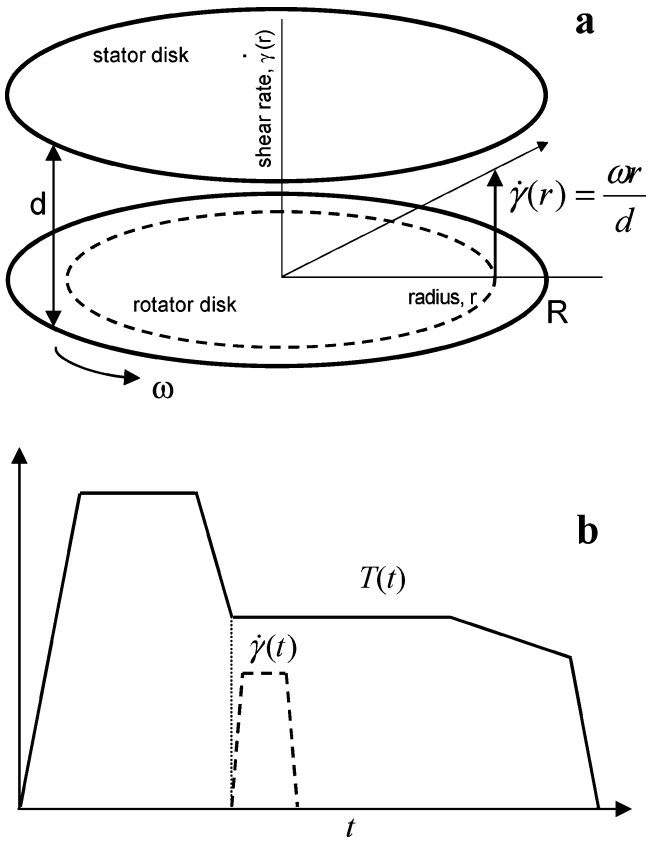

Figure 1. Radial distribution of shear rate in a plate−plate geometry shearing device (a) ($\dot{\gamma} = \omega r/d$, where ω is the angular velocity of the rotator disk, r is the radial position on the disk, and d is the gap between the shear disks); R is the radius of the shearing disks, and therefore, the maximum shear rate achievable in an experiment is $\dot{\gamma}_{max} = \omega R/d$ and schematic time scale of temperature−shear protocol used in this study (b).

Keller[1] may have been among the first to stress the possibility that long chains form the shish, which subsequently helps to nucleate the kebabs via incorporating shorter chains; simulations have supported this view,[20] as have experiments. Time-resolved small-angle scattering of X-rays and light (SAXS, SALS) following flow[21,22] has shown that once an oriented structure has been formed it is pinned by the process of crystallization and persists upon cooling to room temperature. While it has long been established that a small fraction of long chains greatly

* To whom correspondence should be addressed. E-mail: O.Mykhaylyk@sheffield.ac.uk.
† University of Sheffield.
‡ University of Leeds.
§ University of Nottingham.

10.1021/ma702603v CCC: $40.75
Published on Web 02/21/2008

enhances the formation of shish, small-angle neutron scattering studies on labeled blends[23] showed that there is not sufficient time during flow-induced crystallization for long chains to segregate, which suggests that long chains greatly enhance the growth rate of shish, but chains of all lengths become incorporated as the shish grow.

Despite years of work on flow-induced crystallization, many open questions remain: how does the molecular weight distribution influence nucleation rates and morphology? Which are the important molecular time scales (orientation of molecules, retraction of entangled polymers, etc.), and how does the shear rate influence the behavior? As proposed by Keller, is a coil−stretch mechanism at the heart of the enhancement of crystallization in shear?[1] While some of these issues are qualitatively understood, very few quantitative trends are known with confidence. The advent of well-characterized and narrow molecular weight distributions and advanced molecular theories of polymer melts holds the promise of unlocking some of these questions.

This work presents measurements of the critical flow parameters for inducing oriented crystallization using ex-situ SAXS and optical methods. Model linear−linear blends of hydrogenated polybutadienes (h-PBD)[24] were prepared from low-polydispersity polymers of 1700 and 15 kDa (see Supporting Information) with 0.5, 2, and 4 wt % of long chains. The long polymer has a stretch (Rouse) relaxation time of $\tau_R \approx 0.07$ s, which is much longer than the relaxation time of short chains of the matrix polymer, 15 kDa, $\tau_d \approx 70$ μs (see Supporting Information).

A typical protocol for shear-induced crystallization[25] has been used in the experiments (Figure 1b). Disks of polymer were studied in a modified Linkam CSS 450 shear device with a plate−plate geometry. As suggested by previous work,[26] it has been established that the shish are long-lived at temperatures above the melting point of the polymer: it was possible to shear an h-PBD blend 3 K above the end point of the melting curve detectable by differential scanning calorimetry ($T_e = 388$ K), hold it there for 10 h, and still obtain oriented crystals on cooling. Thus, in contrast to most studies of shear-induced crystallization, all shear flows in this study were performed at $T \geq T_e$. The samples were maintained at $T = 433$ K for 15 min to remove flow and crystallinity history[27] and then cooled at a rate of 20 K/min to 388 K, where a pulse of continuous shear was applied followed by a period of isothermal annealing for 1 h at the same temperature. Then the sample was slowly cooled to 363 K at 1 K/min to fully crystallize and finally shock cooled to lower temperatures to enable the complete disk to be unloaded from the cell. Two methods of ex-situ structural characterization were used: SAXS (Bruker AXS Nanostar, Cu-radiation) to measure the orientation of lamellae across the diameter of the samples and optical birefringence measurements by taking images of the disk between a crossed polarizer and analyzer with a simple optical setup comprising a filament source, a collimator, a polarizer, an analyzer, and a CCD camera.

While the sheared samples are turbid at low shear rates and semitransparent at higher shear rates, more details are revealed by polarized light images, which demonstrate a clear boundary between oriented (high shear rate) and unoriented (low shear rate) zones (Figure 2a−d), which correlate with the degree of orientation of the lamellar structure along the flow direction measured by SAXS using the P2 orientation function[28] (Figure 2d). In the outer zone the birefringence, a characteristic Maltese cross, is consistent with lamellae whose chains are parallel to the flow direction. Thus, the macroscopic picture of the lamellae

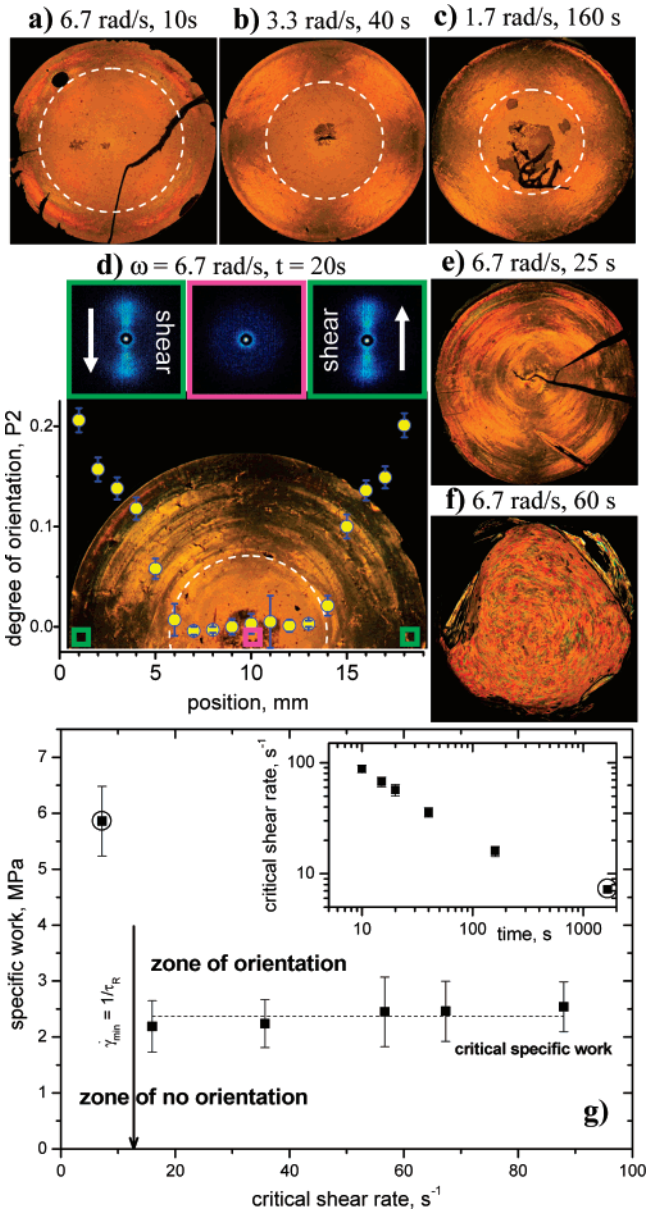

Figure 2. Images of sheared blends of high and low molar mass hydrogenated polybutadiene (2 wt % 1700 kDa in a 15 kDa matrix) taken between crossed polarizer and analyzer. The samples were sheared at 388 K kept for 1 h and then crystallized at lower temperatures (a−f). Some samples (a, e) were damaged on unloading after cooling. The angular velocity (ω in rad/s) and time (t in s) is given at the top of each image, the diameter of the disks is 19 mm, and the gap between shear plates was set to 0.5 mm. The white dashed circles mark a boundary between oriented and nonoriented lamellar structures in the samples. The plot presented over the image (d) shows the degree of orientation of the lamellar structure along the flow direction (function P2) measured across the diameter by SAXS. The color-coded scattering patterns above where taken from the area marked by the green and pink squares. Images e and f demonstrate evolution of elastic turbulence in the sheared samples. (g) A plot of specific work vs measured critical shear rates, $\dot{\gamma}_c$, required for the formation of shish nuclei in the sheared blend. The inset shows how the shear rate required for orientation depends on the shearing time. The dashed line corresponding to the critical specific work divides the plot into areas in which either unoriented or oriented structures can be formed. The arrow indicates the shear rate $\dot{\gamma}_{min} = 1/\tau_R$, where τ_R is the Rouse time of 1700 kDa h-PBD linear molecules, below which the expansion of the long-chain molecules and, subsequently, the formation of oriented nuclei are unlikely.

orientation in the sheared disk resembles, to a certain extent, a slice of a macroscopic spherulite whose core (corresponding to unoriented part of the disk) comprises many very small (and

thus macroscopically disordered) spherulites. The uniaxially oriented SAXS pattern shows a steadily decreasing P2 with decreasing radius until the radius R_c (and corresponding shear rate $\dot{\gamma}_c$) marked by the dashed white line, where both the optical birefringence and the SAXS pattern abruptly become isotropic and consequently P2 tends to zero. The border between zones signifies a critical shear rate $\dot{\gamma}_c$ at which oriented structure forms during the postflow protocol. Hence, polarized light imaging is a simple way to quantify the shear flow parameters that control the morphology of shear-induced polymer crystallization, while the SAXS data provide information about the density of oriented (shish) nuclei formed under shear.

In the majority of in-situ experiments on shear-induced crystallization the structure is measured at a single radius that, for a given angular velocity, defines the shear rate of interest.[21−23,29] Postflow crystallization and subsequent analysis allows the entire radial distribution to be studied. For example, measurements at high strain rate (Figure 2e,f) demonstrate a complicated spiral structure of lamellar orientation. This resembles structures seen in elastic turbulence and observed in polymer solutions[30,31] and may be due to similar physics, as flow deforms the crystallizing melt which is becoming more elastic. Thus, study of the entire sheared disk allows one to observe whether the experimental flows are laminar or unstable. All measurements of the critical shear rate for orientation reported here are from laminar flow regions.

Next the relevance of coil−stretch effects is studied. The critical shear rate $\dot{\gamma}_c$ decreases for longer flow times (inset to Figure 2g), implying that the events that govern orientation occur more rapidly at higher shear rates. This suggests that some measure of the total amount of flow is the governing criterion. Following Janeschitz-Kriegl's hypothesis[32] that the work done on a sheared polymer melt controls the resulting morphology, the specific work w (energy density in Pa = J m^{-3}) can be calculated as follows:

$$w = \int_0^{t_s} \eta[\dot{\gamma}(t)]\dot{\gamma}^2(t)\,\mathrm{d}t \qquad (1)$$

where η is the shear rate dependent viscosity and the integration is over the entire time of shearing t_s. The shear-rate-dependent viscosity was separately measured (see Supporting Information).

For a given flow history, the critical shear rate $\dot{\gamma}_c$ is equivalent to a critical specific work w_c. Intriguingly, this critical work is *independent of shear rate*, with the proviso that the shear rate exceeds the inverse Rouse time for stretching the long chains in the blend, $\dot{\gamma} > \dot{\gamma}_{min} = 1/\tau_R$ (Figure 2g). There was no orientation detected in samples sheared at $\dot{\gamma} < \dot{\gamma}_{min}$, even for applied work a few times higher than the critical specific work. The only orientation detected under these conditions was at the extremities of one sample and is presented as a reference point (Figure 2g, circled point); this is most likely due to secondary flows that occur near the edge of the sample.

The critical work required for orientation decreases with an increasing fraction of high molecular weight molecules and is roughly inversely proportional to the concentration of long-chain molecules in the blends. The specific work for blends with 0.5, 2, and 4 wt % of long-chain polymer are 7.8 ± 2.0, 2.38 ± 0.07, and 0.80 ± 0.13 MPa, respectively. To further assess the criterion of $\dot{\gamma} > 1/\tau_R$ for oriented growth, measurements on a 15 kDa h-PBD melt and a blend with 2 wt % of a 150 kDa linear h-PBD polymer were performed. In both cases there was no molecular oriented structure at the experimentally accessible, shear rates (up to $\dot{\gamma}_{max} = 1000$ s^{-1}). Given the Rouse times of these systems (see Supporting Information), the condition $\dot{\gamma}_{max}\tau_R < 1$ was satisfied, consistent with the lack of formation of oriented shish.

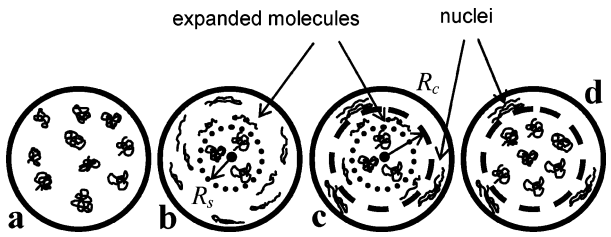

Figure 3. Model of formation of shish nuclei during shear at a constant angular velocity: initial stage or weak shear rates (a), intermediate stage before shish nucleation (b), final stage (c), and after the shear (d). The dotted circle (radius R_s) shows the boundary between zones of nonstretched and stretched long-chain molecules during the shear (isotropic polymers toward the center), and the dashed circle (radius R_c) shows the boundary between the zone of stretched long-chain molecules and the zone of oriented (shish) nuclei formation.

The crucial question is, which molecular features ensures that the specific work provides a clear criterion for the formation of shish kebabs? Upon straining for a time dt the melt experiences a stress $\sigma = \eta\dot{\gamma}$ for a strain $\mathrm{d}\gamma = \dot{\gamma}\,\mathrm{d}t$. A reasonable interpretation of a minimum total work $w = \int\sigma\,\mathrm{d}\gamma$ is as follows: the stress extends the molecules and leads to a higher probability of stretched chain segments. These stretched subchains, which are most abundant at the center of the longest chains, must then find one another to nucleate an oriented object, such as a shish, that remains stable upon cessation of flow. Hence, sufficient advection of stretched subchains must occur to successfully incorporate enough subchains into the shish, which implies a minimum number of strain units. The product of stress and strain can be seen as the joint probability of first producing nucleable objects (stress) and then delivering them together into a nucleus (strain). The specific mechanism of shish formation remains unknown: it could be due to elongation and growth of a single nucleus of stretched subchains or simultaneous incorporation of a long chain into two nuclei that are then advected apart by the flow to stretch the long chain into something resembling a row nucleus.[33] More probable is a combination of these and other microscopic processes. In any case, upon cessation of flow the shear-induced structure must relax very slowly compared to crystallization rates to provide a template for oriented microstructure. Moreover, long shish should be stable above the melting point for typically thin lamellae. This picture agrees with recent results[23] that demonstrate that short chains can participate in, but not initiate, shish formation. It also implies that the critical work is inversely proportional to the concentration of long chains in a bimodal blend, since more long chains require a smaller strain to effect sufficient capture of stretched subchains. Interestingly, the energy density required is 2 orders of magnitude less than thermal energy (k_BT) per long-chain molecule.

One of the most likely scenarios can be readily presented in a cartoon format (Figure 3). The initial state comprises isotropic chains and only the long chains are shown schematically. At low rotational speeds such that $\dot{\gamma} < 1/\tau_R$ at all radii, all chains are unstretched (Figure 3a). At higher rotational speeds and early times (Figure 3b), the long chains outside a radius $R_S = d/(\omega\tau_R)$ (defined by the minimum shear rate $\dot{\gamma}_{min} = 1/\tau_R = R_S\omega/d$) are stretched and noncrystalline (dotted line), while the inner chains are unstretched. The location of this boundary only depends on the angular velocity and the Rouse time of the long chains and defines the minimum shear rate. After a longer time $t > t_N \approx w_c d/(\sigma\omega r)$ (Figure 3c), material outside a radius $R_c(t) = t_N r/t$ (dashed line) at the upper shear rates $\dot{\gamma} > \dot{\gamma}_c = \omega R_c/d$ has

exceeded the work criterion (for example, has experienced sufficient advection of stretched chain portions) and thus contains shish nuclei. The dashed line separates the "stretched zone" from the "shish zone". The material at radii $r < R_S$ inside the shish zone never sees a sufficiently high shear rate to stretch the polymers, and therefore, shish can never be formed. If flow is applied long enough the shish zone vanishes, when $R_c(t) = R_S$, leaving zones of oriented and unoriented (and unstretched) material. Although this process does not exclude the possibility of nucleation of shish from a single stretched molecule as predicted by a theoretical simulation,[34] it should be emphasized that the results presented here clearly indicate the dominant role of shearing time (and therefore strain) on the nucleation of shish that are sufficiently large or well-oriented to produced an oriented structure upon cessation of flow.

The material in the stretched zone and at smaller radii than the shish zone contains stretched molecules that have not had sufficient time to form nuclei, and the chain stretch can relax after flow and prior to the structure being fixed by crystallization. Eventually the stretched zone shrinks and disappears, and upon cooling to induce crystallization only the material in the shish zone forms oriented crystals.

In summary, it has been demonstrated herein that the criterion of specific work of flow to form oriented lamellar (shish-kebab) crystals applies to a model blend, with well-separated time scales in its short and long components. The magnitude of the specific work required to create shish-kebab structures depends on both the chemical structure of the polymer and its molecular weight distribution as both of these parameters affect the Rouse relaxation of the long chains. The criterion has also been tested for several different polydisperse polymers, but for reasons of clarity these will be reported elsewhere. The knowledge of a molecularly informed criterion for the formation of shish-kebab structures in semicrystalline materials has profound implications for the processing and use of polymers in a range of applications from structural automotive parts to food-packaging films and biomedical devices. Judicious combinations of flow geometry, in both molding and extrusion applications, and the molecular weight distribution of the polymer may allow the properties of the final part to be optimized through control of crystallization processes.

Acknowledgment. This work was supported by the EPSRC under Grants GR/ T11852/01 and GR/ T11807/01 and the μPP consortium (http://www.irc.leeds.ac.uk/mupp/), especially Tom McLeish and Christine Fernyhough.

Supporting Information Available: Data on polydispersity of h-PBD used in this study, calculations of relaxation times of the h-PBD molecules, and data on viscosity of the model h-PBD blends. This material is available free of charge via the Internet at http://pubs.acs.org.

References and Notes

(1) Keller, A.; Kolnaar, H. W. Flow induced orientation and structure formation. In *Materials Science and Technology, Processing of Polymers*; Meijer, H. E. M., Ed.; Wiley-VCH: New York, 1997; pp 189−268.
(2) Bashir, Z.; Odell, J. A.; Keller, A. *J. Mater. Sci.* **1986**, *21*, 3993−4002.
(3) McMillan, F. M. *Chain Straighteners-Fruitful Innovation: The Discovery of Linear and Stereoregular Synthetic Polymers;* MacMillan Press: London, 1979; p 207.
(4) Arriola, D. J.; Carnahan, E. M.; Hustad, P. D.; Kuhlman, R. L.; Wenzel, T. T. *Science* **2006**, *312*, 714−719.
(5) Coates, G. W.; Waymouth, R. M. *Science* **1995**, *267*, 217−219.
(6) Guan, Z. B.; Cotts, P. M.; McCord, E. F.; McLain, S. J. *Science* **1999**, *283*, 2059−2062.
(7) Kageyama, K.; Tamazawa, J.; Aida, T. *Science* **1999**, *285*, 2113−2115.
(8) Bent, J.; Hutchings, L. R.; Richards, R. W.; Gough, T.; Spares, R.; Coates, P. D.; Grillo, I.; Harlen, O. G.; Read, D. J.; Graham, R. S.; Likhtman, A. E.; Groves, D. J.; Nicholson, T. M.; McLeish, T. C. B. *Science* **2003**, *301*, 1691−1695.
(9) Blackadder, D. A.; Schleinitz, H. M. *Nature (London)* **1963**, *200*, 778.
(10) Pennings, A. J.; Kiel, A. M. *Kolloid Z. Z. Polym.* **1965**, *205*, 160.
(11) Keller, A. *Rep. Prog. Phys.* **1968**, *31*, 623−704.
(12) Graham, R. S.; Likhtman, A. E.; McLeish, T. C. B. *J. Rheol.* **2003**, *47*, 1171−1200.
(13) Coppola, S.; Grizzuti, N.; Maffettone, P. L. *Macromolecules* **2001**, *34*, 5030−5036.
(14) Elmoumni, A.; Winter, H. H.; Waddon, A. J.; Fruitwala, H. *Macromolecules* **2003**, *36*, 6453−6461.
(15) van Meerveld, J.; Peters, G. W. M.; Hutter, M. *Rheol. Acta* **2004**, *44*, 119−134.
(16) Kumaraswamy, G.; Verma, R. K.; Kornfield, J. A. *Rev. Sci. Instrum.* **1999**, *70*, 2097−2104.
(17) Liedauer, S.; Eder, G.; Janeschitz-Kriegl, H.; Jerschow, P.; Geymayer, W.; Ingolic, E. *Int. Polym. Process.* **1993**, *8*, 236−244.
(18) Macosko, C. W. In *Rheology: Principles, Measurements, and Applications*; VCH Publishers: New York, 1994; pp 83−92.
(19) Ferry, J. D. *Viscoelastic Properties of Polymers*, 3rd ed.; John Wiley & Sons: New York, 1980; p 641.
(20) Wang, M. X.; Hu, W. B.; Ma, Y.; Ma, Y. Q. *Macromolecules* **2005**, *38*, 2806−2812.
(21) Hsiao, B. S. Role of Chain Entanglement Network on Formation of Flow-Induced Crystallization Precursor Structure. In *Progress in Understanding of Polymer Crystallization*; Reiter, G., Strobl, G. R., Eds.; Springer: Berlin, 2007; pp 131−149.
(22) Ogino, Y.; Fukushima, H.; Takahashi, N.; Matsuba, G.; Nishida, K.; Kanaya, T. *Macromolecules* **2006**, *39*, 7617−7625.
(23) Kimata, S.; Sakurai, T.; Nozue, Y.; Kasahara, T.; Yamaguchi, N.; Karino, T.; Shibayama, M.; Kornfield, J. A. *Science* **2007**, *316*, 1014−1017.
(24) Fernyhough, C. M.; Young, R. N.; Poche, D.; Degroot, A. W.; Bosscher, F. *Macromolecules* **2001**, *34*, 7034−7041.
(25) Liedauer, S.; Eder, G.; Janeschitz-Kriegl, H. *Int. Polym. Process.* **1995**, *10*, 243−250.
(26) Zuo, F.; Keum, J. K.; Yang, L.; Somani, R. H.; Hsiao, B. S. *Macromolecules* **2006**, *39*, 2209−2218.
(27) Massa, M. V.; Lee, M. S. M.; Dalnoki-Veress, K. *J. Polym. Sci., Part B: Polym. Phys.* **2005**, *43*, 3438−3443.
(28) Hermans, P. H. *Contribution to the Physics of Cellulose Fibres;* Elsevier: Amsterdam, 1946; p 221.
(29) Nogales, A.; Hsiao, B. S.; Somani, R. H.; Srinivas, S.; Tsou, A. H.; Balta-Calleja, F. J.; Ezquerra, T. A. *Polymer* **2001**, *42*, 5247−5256.
(30) Groisman, A.; Steinberg, V. *Nature (London)* **2000**, *405*, 53−55.
(31) Schiamberg, B. A.; Shereda, L. T.; Hu, H.; Larson, R. G. *J. Fluid Mech.* **2006**, *554*, 191−216.
(32) Janeschitz-Kriegl, H.; Ratajski, E.; Stadlbauer, M. *Rheol. Acta* **2003**, *42*, 355−364.
(33) Seki, M.; Thurman, D. W.; Oberhauser, J. P.; Kornfield, J. A. *Macromolecules* **2002**, *35*, 2583−2594.
(34) Hu, W. B.; Frenkel, D.; Mathot, V. B. F. *Macromolecules* **2002**, *35*, 7172−7174.

MA702603V